YU ISSN 0015—3206
FZKAAA 20 (2) 195 (1988)

ON THE THERMOELECTRIC POWER IN *n*-CHANNEL INVERSION LAYERS ON TERNARY CHALCOPYRITE SEMICONDUCTORS IN THE PRESENCE OF A CLASSICALLY LARGE MAGNETIC FIELD

KAMAKHYA P. GHATAK

Centre of Advanced Study in Radio Physics and Electronics, University of Calcutta, 1, Girish Vydiaratna Lane, Calcutta-700 009, India

NALINAKSHYA CHATTOPADHYAY and MANABENDRA MONDAL

Department of Physics, University College of Science and Technology 92, A. P. C. Road, Calcutta-700 009, India

and

S. BISWAS

Department of Electronics and Telecommunication Engineering, Bengal Engineering College, Howrah-711103, West Bengal, India

Received 28 December 1987

Revised manuscript received 23 May 1988

UDC 538.95

Original scientific paper

An attempt is made to study the thermoelectric power of the carriers in *n*-channel inversion layers on ternary chalcopyrite semiconductors in the presence of a classically large magnetic field under both weak and strong electric field limits, taking *n*-channel inversion layers on $CdGeAs_2$ as an example. It is found, on the basis of newly derived 2D $E - k_s$ dispersion relations of the conduction electrons for both the limits by considering the various types of anisotropies in the energy band, that the same powers increase with decreasing surface electric fields for both the limits and the theoretical expressions are in qualitative agreement with the experimental results. In addition, the corresponding well-known forms for the isotropic two-band Kane model are also obtained from the expressions derived.

1. Introduction

It is well-known that the thermoelectric power, in the presence of a classically large magnetic field (hereafter referred to as TPM), of the electrons in semiconductors is a very important parameter and has also been investigated in the literature under different physical conditions[1-4]. It may also be noted in this context that the TPM is independent of scattering mechanism and in the case of spherical energy surfaces, the shape of the conduction band can be investigated from its experimental determination[3]. Nevertheless, the TPM in n-channel inversion layers on ternary chalcopyrite semiconductors has yet to be investigated for the more interesting case which occurs from the consideration of the various types of anisotropies in the energy spectrum since, in recent years, the inversion layers on semiconductors having non-parabolic and non-standard energy bands are being increasingly studied for their various device oriented applications[5,6] and also since the inversion layers on ternary chalcopyrite semiconductors have been experimentally realized[7]. Besides, the above class of materials are being increasingly used as nonlinear optical materials[8] and light-emitting diodes[9].

It would therefore be of much interest to study the TPM in the n-channel inversion layers on ternary chalcopyrite semiconductors having non-parabolic and non-standard energy bands. Rowe and Shay[10] have demonstrated that the quasi-cubic model[11] can be used to explain the observed splitting and the symmetry properties of the conduction and valence bands at the zone centre in $\vec{k}$-space of the ternary chalcopyrite semiconductors. The s-like conduction band is singly degenerate and the p-like valence band is triply degenerate. Introducing the anisotropic crystal potential to the Hamiltonian, Kildal[12-13] proposed an $E - \vec{k}$ dispersion relation for the carriers in the bulk specimen in the same semiconductor, according to which the conduction band corresponds to a simple ellipsoid of revolution at the zone center in $\vec{k}$-space together with the assumptions of isotropic inter-band momentum matrix element and isotropic spin-orbit splitting, respectively.

In what follows, in Sec. 1, we shall generalize the Kildal model by incorporating the anisotropies in the momentum-matrix element and isotropic spin-orbit splitting parameters, respectively, since the anisotropies in the two above mentioned band parameters are significant physical features for the above class of materials[14]. We shall formulate the TPM's in n-channel inversion layers on ternary chalcopyrite semiconductors for both weak and strong electric field limits, by deducing the appropriate 2D electron energy spectrums. In Sec. 1.2 we shall obtain the corresponding results for three-band Kane model and that of two-band Kane model, respectively, from our generalized expressions under certain limiting conditions. We shall take n-channel inversion layers on $CdGeAs_2$ as an example for the purpose of numerical computations.

2. Theoretical background

2.1. *Formulation of band structure and the subsequent derivation of the 2D-TPM's in n-channel inversion layers on ternary chalcopyrite semiconductors*

The form of $\vec{k}\cdot\vec{p}$ matrix for ternary chalcopyrite semiconductors can be written, following Kildal[1,2], as

$$H = \begin{bmatrix} H_1 & H_2 \\ H_2^+ & H_1 \end{bmatrix} \tag{1}$$

where

$$H_1 \equiv \begin{bmatrix} E_g & P_{||}\,k_z & 0 & 0 \\ P_{||}\,k_z & -\left(\delta + \frac{\Delta_{||}}{3}\right) & \frac{\sqrt{2}}{3}\Delta_{\perp} & 0 \\ 0 & \frac{\sqrt{2}}{3}\Delta_{\perp} & -\frac{2}{3}\Delta_{||} & 0 \\ 0 & 0 & 0 & 0 \end{bmatrix}, \quad H_2 \equiv \begin{bmatrix} 0 & 0 & x_{,-} & x_{,+} \\ 0 & 0 & 0 & 0 \\ -x_{,-} & 0 & 0 & 0 \\ x_{,+} & 0 & 0 & 0 \end{bmatrix},$$

E_g is the band gap, $P_{||}$ and $P_{\perp}$ are the momentum-matrix elements parallel and perpendicular to the c-axis, respectively, $\Delta_{||}$ and $\Delta_{\perp}$ are the spin-orbit splitting parameters parallel and perpendicular to the direction of crystal axis, respectively, δ is the crystal-field splitting parameter, $x_{,\perp} = (k_x \pm \mathrm{i}\,k_y)\frac{P_{\perp}}{\sqrt{2}}$ and $\mathrm{i} \equiv \sqrt{-1}$.

Thus neglecting the contribution of the higher bands and the free-electron term the diagonalization of the above matrix leads to the dispersion relation of the conduction electrons in bulk specimens of ternary chalcopyrite semiconductors as

$$[p_s^2/2M_{\perp}\,V(\varepsilon)] + [p_z^2/2M_{||}] = \varphi(\varepsilon) \tag{2}$$

where $p_s \equiv \hbar\,k_s$, $\hbar \equiv h/2\pi$, h is the Planck's constant, $k_s^2 \equiv k_x^2 + k_x^2$, $M_{\perp,||} = m^*_{\perp,||}(E_g + 2\,\Delta_{||,\perp}/3)$. $(E_g + \Delta_{\perp,||})^{-1}$, $m^*_{\perp}$ and $m^*_{||}$ are the transverse and longitudinal effective electron masses, respectively, at the edge of the conduction band, $p_z \equiv \hbar\,k_z$,

$$V(\varepsilon) \equiv (\varepsilon + E_g)\left(\varepsilon + E_g + \frac{2}{3}\Delta_{||}\right)\left[(\varepsilon + E_g)\left(\varepsilon + E_g + \frac{2}{3}\Delta_{||}\right) + \right.$$

$$\left. + \delta\left(\varepsilon + E_g + \frac{\Delta_{||}}{3}\right) + \frac{1}{9}(\Delta_{||}^2 - \Delta_{\perp}^2)\right],$$

$$\varphi(\varepsilon) \equiv U(\varepsilon)/V(\varepsilon),$$

$$U(\varepsilon) \equiv \left\{\varepsilon(1 + \alpha\,\varepsilon)\left[(\varepsilon + E_g)(\varepsilon + E_g + \Delta_{||}) + \delta\left(\varepsilon + E_g + \frac{2}{3}\Delta_{||}\right) + \right.\right.$$

$$\left.\left. + \frac{2}{9}(\Delta_{||}^2 - \Delta_{\perp}^2)\right]\right\}\left[(\varepsilon + E_g)\left(\varepsilon + E_g + \frac{2}{3}\Delta_{||}\right) + \right.$$

$$\left. + \delta\left(\varepsilon + E_g + \frac{\Delta_{||}}{3}\right) + \frac{1}{9}(\Delta_{||}^2 - \Delta_{\perp})\right]$$

and $$\alpha \equiv 1/E_g.$$

Thus, using Eq. (2) and following the method as given in Refs. 5 and 14 the modified 2D electron energy spectra in n-channel inversion layers on the above class of materials can, respectively, be expressed, both under weak and strong electric field limits, as

$$X(E) = a(E)\, p_s^2 (M_\perp)^{-1} + S_n [\hbar\, e\, F_s\, Y(E)]^{2/3} \tag{3a}$$

and

$$\varphi(E) = [p_s^2/2M_\perp\, V(E)] + \left[\frac{4}{3} S_n^{3/2} \hbar\, e\, F_s \sqrt{\omega(E)} \sqrt{2E_g M_{||}}\right] \tag{3b}$$

where E is the electron energy as measured from the edge of the conduction band at the surface, F_s is the surface electric field applied perpendicular to the surface and parallel to the c-axis, n ($\equiv 0,1,2,\ldots$) is the electric subband index and S_n are the zeros of Airy functions[15] [$Ai(-S_n) = 0$]. Besides, the functions $X(E)$, $Y(E)$, $\varphi(E)$ and $\omega(E)$ are defined in Appendix A.

Using Eqs. (3a, b), the density-of states functions for both the limits can, respectively, be expressed as

$$\varrho_\omega(E) = (M_\perp/2\pi\hbar^2) \sum_{n=0}^{n_{max}} g(E)\, H(E - E_\omega) \tag{4a}$$

and

$$\varrho_s(E) = (M_\perp/\pi\hbar^2) \sum_{n=0}^{n_{max}} I(E)\, H(E - E_s) \tag{4b}$$

where H is the Heaviside step function and the symbols $g(E)$, E_ω, $I(E)$ and E_s are defined in Appendix A. Thus combining (4a, b) with the Fermi-Dirac occupation probability factor $f_0(\varepsilon)$, the expressions for the surface electron concentration per unit area under weak and strong electric field limits can, respectively, be written as

$$N_{s\omega} = (M_\perp/2\pi\hbar^2) \sum_{n=0}^{n_{max}} [p(E_{F\omega}) + q(E_{F\omega})] \tag{5a}$$

and

$$N_{ss} = (M_\perp/\pi\hbar^2) \sum_{n=0}^{n_{max}} [r(E_{Fs}) + \mathscr{S}(E_{Fs})] \tag{5b}$$

where E_F is the Fermi energy under low-electric-field limit as measured from the edge of the conduction band at the surface and E_{Fs} is the corresponding energy under high-electric-field limit. Besides, the function $p(E_{F\omega})$, $q(E_{F\omega})$, $r(E_{Fs})$ and $\mathscr{S}(E_{Fs})$ are defined in the Appendix A.

Incidentally, the TPM of the 2D electrons in inversion layers on semiconductors can be expressed[4] as

$$S = (eT)^{-1} \left[\left\{\sum_{n=0}^{n_{max}} \int_{E'}^{\infty} E\, A_0(E) \frac{\partial f_0(E)}{\partial E}\, dE\right\} \times \left\{\sum_{n=0}^{n_{max}} \int_{E'}^{\infty} A_0(E) \frac{\partial f_0(E)}{\partial E}\, dE\right\}^{-1} - E_F\right] \tag{6}$$

where $A_0(E)$ is the area of the 2D k_s space and E' can be determined from the equation $A_0(E') = 0$. Thus combining Eqs. (3a), (3b) and (6) the expressions for the TPM under weak and strong electric field limits can, respectively, be expressed as

$$S_\omega = \frac{1}{eT}\left[\frac{\sum_{n=0}^{n_{max}} [P(E_{F\omega}) + Q(E_{F\omega})]}{\sum_{n=0}^{n_{max}} [p(E_{F\omega}) + q(E_{F\omega})]} - E_{F\omega}\right] \tag{7a}$$

and

$$S_s = \frac{1}{eT}\left[\frac{\sum_{n=0}^{n_{max}} [R(E_{Fs}) + S(E_{Fs})]}{\sum_{n=0}^{n_{max}} [r(E_{Fs}) + \mathscr{S}(E_{Fs})]} - E_{Fs}\right] \tag{7b}$$

where

$$P(E_{F\omega}) = E_{F\omega}\, p(E_{F\omega}), \quad Q(E_{F\omega}) \equiv \sum_{t=1}^{t_0} \nabla_t [P(E_{F\omega})], \quad R(E_{Fs}) \equiv E_{Fs}\, r(E_{Fs}) \quad \text{and}$$

$$S(E_{Fs}) \equiv \sum_{t=1}^{t_0} \nabla_t [R(E_{Fs})].$$

2.2. *Special cases*

a) Under the substitutions $\delta = 0$, $\Delta_{\|} = \Delta_{\perp} = \Delta$ (the isotropic spin-orbit splitting parameter) and $m_{\|}^* = m_{\perp}^* = m_0^*$ (the isotropic effective electron mass at the edge of the conduction band) and $\delta = 0$, Eqs. (2), (3a) and (3b) assume the forms

$$\frac{\hbar^2 k^2}{2m_0^*} = \gamma(\varepsilon), \quad \gamma(\varepsilon) \equiv \frac{\left(E_g + \frac{2}{3}\Delta\right)\varepsilon(\varepsilon + E_g)(\varepsilon + E_g + \Delta)}{E_g(E_g + \Delta)\left(\varepsilon + E_g + \frac{2}{3}\Delta\right)} \tag{8}$$

$$\gamma(E) = (\hbar^2 k_s^2/2m_0^*) + S_n [\hbar e F_s \psi(E)(2m_0^*)^{-1/2}]^{2/3} \tag{9a}$$

and

$$\gamma(E) = (\hbar^2 k_s^2/2m_0^*) + S_n^{3/2}\left[\frac{4}{3}\hbar e F_s \sqrt{L(E)}(2E_g m_0^*)^{-1/2}\right] \tag{9b}$$

where the symbols $\psi(E)$ and $L(E)$ are defined in Appendix B. It must be mentioned that Eq. (8) is the standard dispersion relation of the conduction electrons in bulk specimens of Kane-type semiconductors and is known as three-band Kane model[16]. It is thus expected that, under these substitutions, the results derived in this paper should convert into simpler forms for inversion layers on semiconductors whose energy band structures are defined by three band Kane model. Under the substitutions, as mentioned above, the basic forms of equations (4a—7b) will not be changed. The different meaning of the various symbols in equations (4a—7b) as appropriate for inversion layers on semiconductors whose energy band structures are defined by three-band Kane model are written in the Appendix B.

b) Under the substitutions $\Delta \to \infty$ and $S_n \to [3\pi(4n+3)/8]^{2/3}$ (for large values of n)[15] in the above equations, the expressions for the dispersion relation, the electron concentration and TPM in n-channel inversion layers on Kane-type semiconductors whose energy band structures are defined by two-band Kane model can, respectively, be expressed, for both the limits, as

$$\varepsilon(1+\alpha\varepsilon) = (\hbar^2 k^2/2m_0^*) \tag{10}$$

$$E(1+\alpha E) = (\hbar^2 k_s^2/2m_0^*) + \left[\frac{3}{2}\hbar e F_s \pi \left(n+\frac{3}{4}\right)(1+2\alpha E)(2m_0^*)^{-1/2}\right]^{2/3} \tag{11a}$$

$$E(1+\alpha E) = (\hbar^2 k_s^2/2m_0^*) + \left[2\pi\hbar e F_s \left(n+\frac{3}{4}\right)(2m_0^* E_g)^{-1/2}\right] \tag{11b}$$

$$N_{s\omega} = (m_0^* k_B T/\pi\hbar^2)\sum_{n=0}^{n_{max}}[\Theta(\eta_{l\omega}) + \varrho(\eta_{l\omega})] \tag{12a}$$

$$N_{ss} = (m_0^* k_B T/\pi\hbar^2)\sum_{n=0}^{n_{max}}[I(\eta_{ls}) + \tau(\eta_{ls})] \tag{12b}$$

$$S_\omega = (k_B/e)\left[\frac{\sum_{n=0}^{n_{max}}[\beta(\eta_{l\omega}) + \delta(\eta_{l\omega})]}{\sum_{n=0}^{n_{max}}[\Theta(\eta_{l\omega}) + \varrho(\eta_{l\omega})]} - \eta_\omega\right] \tag{13a}$$

$$S_s = (k_B/e)\left[\frac{\sum_{n=0}^{n_{max}}[G(\eta_{ls}) + H(\eta_{ls})]}{\sum_{n=0}^{n_{max}}[I(\eta_{ls}) + \tau(\eta_{ls})]} - \eta_s\right] \tag{13b}$$

where the notations are defined in Ref. 4. It may be noted in this context that Eq. (11a, b) were derived for the first time by Antcliffe et al.[5]. Besides Eqs. (12a to 13b) were derived for the first time by Ghatak and Mondal[4].

3. Results and discussion

Using equations (5a and 7a) together with the parameters[19,20] $m_{\|} = 0.030\, m_0$, $m_\perp^* = 0.039\, m_0$, $\Delta_{\|} = 0.34$ eV, $\Delta_\perp = 0.36$ eV, $\delta = -0.21$ eV, $E_g = 0.57$ eV and $\varepsilon_{sc} = 14.3\,\varepsilon_0$ as appropriate for $CdGeAs_2$ we have plotted the TPM under the weak-electric field limit at 4.2 K for n-channel inversion layers on $CdGeAs_2$ as a function of the surface electric field at the electric quantum limit, as shown in curve a of Fig. 1, in which the dotted curve also exhibits the same dependence by using the experimental values of the thermoelectric power of the electrons in n-

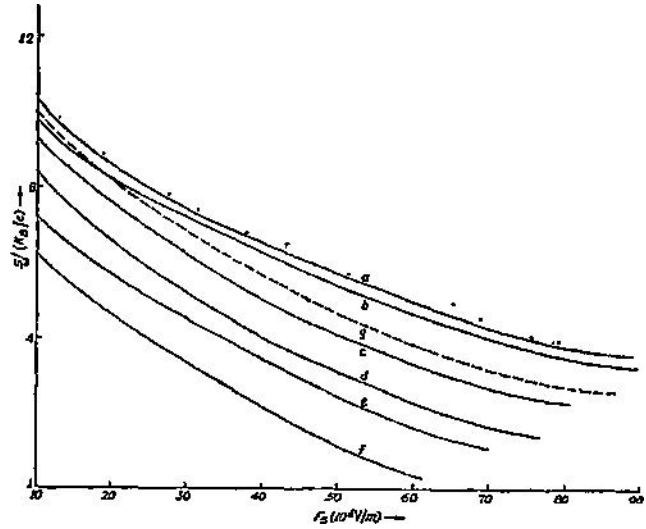

Fig. 1. Plot of the normalized TPM in the electric quantum limit as a function of the surfac electric field under low electric field limit in n-channel inversion layers on n-$CdGeAs_2$ by using (a) the proposed dispersion relation at 4.2 K, (b) the same relation at 20 K, (c) the isotropic three band Kane model at 4.2 K, (d) the same model at 20 K, (e) the isotropic two band Kane model at 4.2 K, (f) the same model at 20 K and (g) in the absence of crystal field splitting parameter at 4.2 K. The dotted plot exhibits the experimental datas.

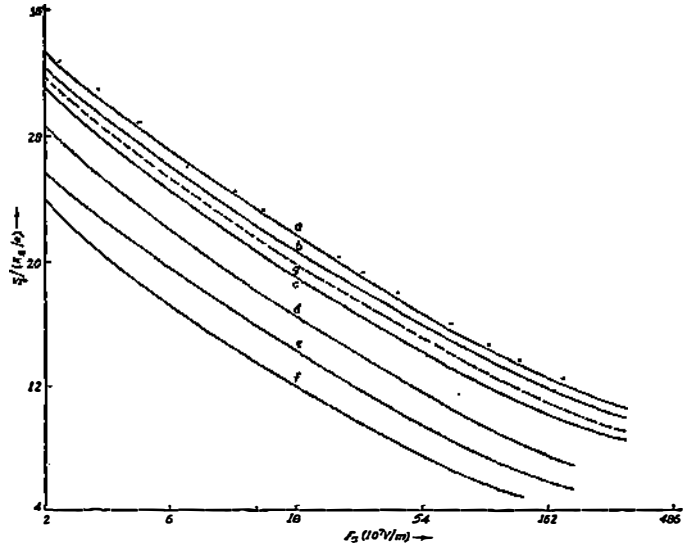

Fig. 2. Plot of the normalized TMP in the electric quantum limit as a function of the surface electric field under high electric field limit in n-channel inversion layers on n-$CdGeAs_2$ by using (a) the proposed dispersion relation at 4.2 K, (b) the same relation at 20 K, (c) the isotropic three band Kane model at 4.2 K, (d) the same model at 20 K, (e) the isotropic two-band Kane model at 4.2 K, (f) the same model at 20 K, (g) in the absence of crystalline field spliting parameter at 4.2 K. The dotted plot exhibits the experimental datas.

channel inversion layers on $CdGeAs_2$ under the weak-electric field limit in the presence of a classically large magnetic field as given elsewhere[17]. Using the appropriate equations the plots corresponding to the 3-band Kane model and the 2-band Kane model of n-channel inversion layers of n-$CsGeAs_2$, with an effective electron mass ($m_t^* = 0.02\, m_0$) which of the order of the mass at the edge of the conduction band of n-$CdGeAs_2$[13] and taking $\Delta = 0.35$ eV (for the purpose of numerical computations in the 3-band Kane model), are also shown in Fig. 1, in which the curve g corresponds to $\delta = 0$. The plots b, d and f in Fig. 1 exhibit the corresponding dependences at 20 K. Using the same parameters as used in obtaining the Fig. 1 and using (5b) and (7b) we have plotted the TPM under the strong-electric-field limit at 4.2 K, as shown by curve a of Fig. 2, in which the dashed also exhibits the same dependence by using the experimental values of the thermoelectric power of the electrons in n-channel inversion layers on $CdGeAs_2$ under the strong-electric-field limit in the presence of a classically large magnetic-field at the electric quantum limit. Besides the plots for the various simplified limiting cases have further been considered in Fig. 2.

It appears from both the figures that the TPM's decrease with increasing surface electric field, and are in good qualitative agreement with the experimental datas. It is also seen that the tetragonal crystal field affects TPM of the electrons quite significantly in n-channel inversion layers of ternary chalcopyrite semiconductors for relatively large values of the surface electric field. Furthermore, for a fixed value of the surface electric field, TPM of the electrons, is larger as compared to that in the absence of crystalline field effects in the whole range of fields considered for both the limits. Though TPM also increases nonlinearly with surface field for both the limits in various other limiting cases, the rates of increase are different from that in the proposed band model.

It is worth remarking to note that if the direction of application of the surface electric field applied perpendicular to the surface is taken as one of the transverse directions and not as a longitudinal one, as assumed in the present, the TPM's would different be analytically for both the limits. Nevertheless, the arbitrary choice of the direction normal to the surface would not result in a change of the basic qualitative feature of TPM in n-channel inversion layers on ternary chalcopyrite semiconductors. Since most of the carriers occupy the lowest electric subband at low temperatures for which the effects of electric quantization become more pronounced, it is sufficiently accurate for such temperatures to consider the occupation of the lowest electric subband[18]. We note that though the many-body effects, the hot-electron effects, the formation of band tails, arbitrary orientation of the direction of electric quantization, the effects of surface states and the occupancy of the electrons in the electric subbands above the lowest one have been neglected in the theoretical formulation this simplified triangular-potential well approximation exhibits the basic qualitative features of TPM in n-channel inversion layers on semiconductors and the agreement between the theory and the experimental results becomes rather significant for both the limits in spite of the above simplifications.

The general features of the effects of surface electric field on the TPM in n-channel inversion layers as discussed here would also be valid for most of the inversion layers on small-gap semiconductors since these semiconductors have non-parabolic energy bands obeying Kane's dispersion relation whereas the pre-

sent analysis is based on generalized Kane's theory. Finally it may be remarked that the basic purpose of the present paper is not solely to investigate the TPM's in n-channel inversion layers on ternary chalcopyrite semiconductors but also to formulate for the first time the generalized 2D electron dispersion relations by including the various types of anisotropies in the energy spectrum for both the limits since the various transport phenomena and the derivation of the expressions for many important physical parameters of 2D semiconductors devices are based on the carrier dispersion relation in such materials.

Appendix A

The functions $X(E)$, $Y(E)$, $\varphi(E)$, $\omega(E)$, $g(E)$, E_ω, $I(E)$, E_s, $p(E_{F\omega})$, $q(E_{F\omega})$, $r(E_{Fs})$ and $\mathscr{S}(E_{Fs})$, are defined as follows:

$$X(E) = 2\,U(E)\,a(E) \tag{A1}$$

$$a(E) = M_{\|}\,[V(E)]^{-1} \tag{A2}$$

$$Y(E) = 2a(E)\,[\overline{\varrho}(E)] \tag{A3}$$

$$\omega(E) = \left[(E + E_g)\left(E + E_g + \frac{2}{3}\Delta_{\|}\right)\right]^{-1}\left[(E + E_g + \Delta_{\|}) + \right.$$

$$\left. + \delta\left(E + E_g + \frac{2}{3}\Delta_{\|}\right) + \frac{2}{9}(\Delta_{\|}^2 - \Delta_{\perp}^2)\right] \tag{A4}$$

$$g(E) = \{a^{-1}(E)\,[X_1(E) - \frac{2}{3}\,Y_1(E)\,Y^{-1/3}(E)\,S_n\,(\hbar\,e\,F_s)^{2/3}] -$$

$$- a_1(E)\,a^{-2}(E)\,[X(E) - S_n\,\{\hbar\,e\,F_s\,Y(E)\}^{2/3}]\} \tag{A5}$$

$$X(E_\omega) - S_n\,[\hbar\,e\,F_s\,Y(E_\omega)]^{2/3} = 0 \tag{A6}$$

$$I(E) = [V(E)\,\{\varphi_1(E) - \frac{2}{3}\hbar\,e\,F_s\,S_n^{3/2}\,\omega_1(E)\,[2M_{\|}\,E_g\,\omega(E)]^{-1/2}\} +$$

$$+ V_1(E)\,\{\varphi(E) - \frac{4}{3}\hbar\,e\,F_s\,S^{3/2}\,[\omega(E)/2E_g\,M_{\|}]^{1/2}\}] \tag{A7}$$

$$\varphi(E_s) - \frac{4}{3}\hbar\,e\,F_s\,S_n^{3/2}\,[\omega(E_s)/2E_g\,M_{\|}]^{1/2} = 0 \tag{A8}$$

$$p(E_{F\omega}) = (\{a^{-1}(E)\,\{X(E) - S_n\,[\hbar\,e\,F_s\,Y(E)]^{2/3}\}\})\big|_{E=E_{Fs}} \tag{A9}$$

$$q(E_{F\omega}) = \sum_{t=0}^{t_0} \nabla_t [p(E_{F\omega})] \tag{A10}$$

$$r(E_{Fs}) = \left\{ V(E) \left[\varphi(E) - \frac{4}{3} \hbar e F_s S_n^{3/2} \left(\frac{(\omega(E)}{2E_g M_{\|}} \right)^{1/2} \right] \right\} \Big|_{E=E_{Fs}} \tag{A11}$$

$$\mathscr{S}(E_{Fs}) = \sum_{t=1}^{t_0} \nabla_t [r(E_{Fs})] \tag{A12}$$

where

$$\bar{\varrho}(E) = U(E) \Big\{ (1 + 2\alpha E) [E(1 + \alpha E)]^{-1} + (E + E_g + \Delta_{\|})^{-1} -$$

$$- \tau(E) [I_0(E)]^{-1} - \left(E + E_g + \frac{2}{3} \Delta_{\|} \right)^{-1} \Big\},$$

$$\tau(E) \equiv I_0(E) \{ C(E) [1 + A(E)]^{-1} - H(E) [1 + G(E)]^{-1} \},$$

$$I_0(E) \equiv [1 + A(E)] [1 + G(E)]^{-1},$$

$$A(E) \equiv [\delta \left(E + E_g + \frac{2}{3} \Delta_{\|} \right) + \frac{2}{9} (\Delta_{\|}^2 - \Delta_{\perp}^2)] \times [(E + E_g)(E + E_g + \Delta_{\|})],$$

$$G(E) \equiv \left[(E + E_g) \left(E + E_g + \frac{2}{3} \Delta_{\|} \right) \right]^{-1} \left[\frac{1}{9} (\Delta_{\|}^2 - \Delta_{\perp}^2) + \delta \left(E + E_g + \frac{1}{3} \Delta_{\|} \right) \right],$$

$$C(E) \equiv A(E) \{ \delta [\delta \left(E + E_g + \frac{2}{3} \Delta_{\|} \right) + \frac{2}{9} (\Delta_{\|}^2 - \Delta_{\perp}^2)]^{-1} -$$

$$- (2E + 2E_g + \Delta_{\|}) [(E + E_g)(E + E_g + \Delta_{\|}]^{-1} \},$$

$$H(E) \equiv G(E) \Big\{ \delta \Big[\delta \left(E + E_g + \frac{\Delta_{\|}}{3} \right) + \frac{1}{9} (\Delta_{\|}^2 - \Delta_{\perp}^2) \Big]^{-1} -$$

$$- \left(2E + 2E_g + \frac{2}{3} \Delta_{\|} \right) \left[(E + E_g) \left(E + E_g + \frac{2}{3} \Delta_{\|} \right) \right]^{-1} \Big\},$$

$$\nabla_t \equiv 2 (k_B T)^{2t} (1 - 2^{1-2t}) \zeta(2t) \frac{\mathrm{d}^{2t}}{\mathrm{d}E_F^{2t}},$$

k_B is Boltzmann constant, T is the temperature, t is the set of real positive integers, $\zeta(2t)$ is the zeta function of order $2t$, $\mathrm{d}/\mathrm{d}E [f(E)] \equiv f_1(E)$ where $f(E)$ is any differentiable function of energy.

Appendix B

The function $\varphi(E)$, $L(E)$, $g(E)$, $\gamma(E_\omega)$, $I(E)$, $\gamma(E_s)$, $p(E_{F\omega})$, $q(E_{F\omega})$, $r(E_{Fs})$ and $\mathscr{S}(E_{Fs})$, for the 3-band Kane model are defined as follows

$$\varphi(E) = L(E)\left\{(1 + 2\alpha E) + E(1 + \alpha E)\left[(E + E_g + \Delta)^{-1} - \right.\right.$$

$$\left.\left. - (E + E_g + \frac{2}{3}\Delta)^{-1}\right\}\right] \tag{B1}$$

$$L(E) = \gamma(E)\,[E(1 + \alpha E)]^{-1} \tag{B2}$$

$$g(E) = [M_\perp/2m_0^*]\,\{\gamma_1(E) - \frac{2}{3} S_n \psi^{-1/3}(E)\,\psi_1(E)\,[\hbar e F_s (2m_0^*)^{-1/2}]^{2/3} \tag{B3}$$

$$\gamma(E_\omega) - S_n\,[\hbar e F_s \psi(E_\omega)(2m_0)^{-1/2}]^{2/3} = 0 \tag{B4}$$

$$I(E) = (M_\perp/m_0^*)\,\{\gamma_1(E) - \frac{2}{3} S_n^{2/3} \hbar e F_s L_1(E)\,[2E_g m_0^* L(E)]^{-1/2}\} \tag{B5}$$

$$\gamma(E_s) - S_n^{2/3}\left[\frac{4}{3}\hbar e F_s \sqrt{L(E_s)}\,(2m_0^* E_g)^{-1/2}\right] = 0 \tag{B6}$$

$$p(E_{F\omega}) = \gamma(E_{F\omega}) - S_n\,[\hbar e F_s \psi(E_{F\omega})(2m_0^*)^{-1/2}]^{2/3} \tag{B7}$$

$$q(E_{F\omega}) = \sum_{t=1}^{t_0} V_t\,[p(E_{F\omega})] \tag{B8}$$

$$r(E_{Fs}) = \gamma(E_{Fs}) - S_n^{3/2}\left[\frac{4}{3}\hbar e F_s \sqrt{L(E_{Fs})}\,(2E_g m_0^*)^{-1/2}\right] \tag{B9}$$

$$\mathscr{S}(E_{Fs}) = \sum_{t=1}^{t_0} V_t\,[r(E_{Fs})] \tag{B10}$$

References

1) W. Zawadzki, Adv. Phys. **23** (1974) 435;
2) S. P. Zelenin, A. S. Kondratev and A. I. Kuchma, Sov. Phys. Semicond. **16** (1982) 355;
3) I. M. Tsidilkovski, Band *Structure of Semiconductors*, Pergamon Press, Oxford, p. 313 (1982) and the references cited therein.
4) K. P. Ghatak and M. Mondal, Phys. Stat. Sol. (b) **135** (1986) 819;
5) G. A. Anticliffe, R. T. Bate and R. A. Reynolds, Proc. Int. Conf. Phys. of Semimetals and Narrow-Gap Semiconductors, ed. D. L. Carter and R. T. Bates, Pergamon Press, Oxford, p. 499 (1971);

6) T. Ando, A. H. Fowler and F. Stern, Rev. Mod. Phys. **54** (1982) 432 and the references cited therein;
7) V. B. Lazarev, V. Ya. Shevchenko and S. F. Marenkin, Izv. Acad. Nauk. USSR Nearg. Matev. **15** (1979) 1707;
8) D. S. Chemla, P. J. Kupeck, D. S. Robertson and R. C. Smith, Opt. Commun. **3** (1971) 29;
9) J. L. Shay, K. J. Beckmann, E. Buehyler and J. H. Wernick, Appl. Phys. Lett. **226** (1973) 23;
10) J. W. Rowe and J. L. Shay, Phys. Rev. **83** (1971) 451;
11) J. J. Hopfield, J. Phys. Chem. Solids **15** (1960) 97;
12) H. Kildal, Phys. Rev. **B10** (1974) 5082;
13) J. L. Shay and J. H. Warnick, *Ternary Chalcopyrite Semiconductors: Growth, Electronic Properties and Applications*, Pergamon Press London (1975);
14) G. Paasch, T. Fiedler, M. Kolar and I. Bartos, Phys. Stat. Solidi (b) **118** (1983) 641;
15) M. Abramowitz and I. A. Stegun, *Handbook of Mathematical Functions*, Dover, New York (1965);
16) V. A. Vil'kotskii, D. S. Domanevskii, R. D. Kakanov and V. V. Krasovskii, Sov. Phys. Semicond. **13** (1979) 553;
17) S. I. Radautsan, E. A. Arushanov, A. N. Nateprov and G. P. Chuika, Cadmium Arsenide and Phosphide (Kishinev, USSR, 1976);
18) Z. A. Weinberg, Solid State Electronics **20** (1977) 11;
19) B. R. Nag, *Electron Transport in Compound Semiconductors*, Springer-Verlag, 1980;
20) M. Neuberger, *Electronic Materials*, Vol. 2, Plenum Data Corporation, New York, 1971.

O TERMOELEKTRIČNOM NAPONU U *n*-KANALNIM INVERZNIM SLOJEVIMA NA TERNARNIM KALKOPIRITNIM POLUVODIČIMA U PRISUSTVU KLASIČNO JAKIH MAGNETSKIH POLJA

KAMAKHYA P. GHATAK

Centre of Advanced Study in Radio Physics and Electronics, University of Calcutta, 1, Girish Vidyaratna Lane, Calcutta — 700 009, India

NALINAKSHYA CHATTOPADHYAY i MANABENDRA MONDAL

University College of Science and Technology, 92, A. P. C. Road, Calcutta — 700 009, India

i

S. BISWAS

Department of Electronics and Telecommunication Engineering, Bengal Engineering College, Howrah — 711103, West Bengal, India

UDK 538.95

Originalni znanstveni rad

Razmatran je termoelektrični napon nosilaca naboja u *n*-kanalnim inverznim slojevima na ternarnim kalkopiritnim poluvodičima u prisustvu klasično jakog magnetskog polja. To je učinjeno za limes jakog i slabog električnog polja, uzevši kao primjer *n*-kanalne inverzne slojeve na $CdGeAs_2$. Na osnovu nedavno izvedene 2D $E - k_s$ disperzione relacije za vodljive elektrone a uzevši u obzir različite tipove anizotropije u energetskoj vrpci, nađeno je da napon raste s padom površinskog električnog polja u oba limesa. Također, teorijski izrazi su u kvalitativnom slaganju s eksperimentalnim rezultatima.